MULTISCALE CLIMATE VARIABILITY IN THE ASIAN PACIFIC

V.I. Ponomarev[1], V.V. Krokhin[2], D.D. Kaplunenko[1], A.S. Salomatin[1]

[1] *V.I. Il'ichev Pacific Oceanological Institute, Far Eastern Branch of Russian Academy of Sciences (POI FEBRAS), Russia*
Email: ponomarev@poi.dvo.ru

[2] *Far Eastern Regional Hydrometeorological Research Institute (FERHRI), Russia*

The paper describes major patterns of centennial/semi-centennial climatic tendencies and oscillations in the surface air temperature and precipitation for the Northeast Asia in the 20th century, as well as, in the sea surface temperature (SST) for the Northwest Pacific in the second half of the century. Linear trend of monthly mean precipitation and air/water temperature is estimated by two statistical methods. The first one is the least squares method with the Fisher's test for a significance level. The second method is a nonparametric robust method based on the Theil's rank regression and the Kendall's test for a significance level applicable to the dataset with the abnormal distribution function typical for the precipitation time series. Differences of the trend in precipitation estimated by two methods are shown. Regional features of climate change and dominating oscillations associated with cooling or warming, positive or negative precipitation anomalies in different seasons and large-scale areas are found. High seasonality of both climatic trends and the low frequency variability in the studied area are revealed. It is shown that the semi-centennial summer cooling in a central continental area of Asia accompanies the semi-centennial negative SST anomaly in the offshore region of the western subarctic pacific gyre. At the same time, warming at Kamchatka Peninsula and marginal subtropic area of the Northeast Asia accompanies the positive SST trend in the Kuroshio and Aleutian current systems. Similar alternation and seasonality of positive and negative temperature anomalies are also typical for the El Niño signal in the Northwest Pacific SST.

INTRODUCTION

Recent examination of global and hemisphere changes in the annual mean surface air temperature, precipitation (Bradley *et al*., 1986; Vinnikov *et al*., 1990) and SST (Folland *et al*., 2001; Casey and Cornillon, 2001) in the 20th century has shown the statistically significant global warming (Vinnikov *et al*., 1990; Folland *et al*., 2001; Izrael *et al*., 2001) and precipitation increase in the latitude band of 35–70°N over land areas (Bradley *et al*., 1986; Vinnikov *et al*., 1990). It is increasing in the late 20th century and dominating in moderate latitudes and subarctic zone (Folland *et al*., 2001; Kondratiev and Demirchan, 2001).

Regional climatic tendencies in annual/seasonal mean air temperature in Russia (Rankova and Gruza, 1998; Varlamov *et al*., 1998) and countries situated in the East Asia (Tyson *et al*., 2002) are in agreement with major conclusions on climate change in the northern hemisphere mentioned above. At the same time, it was shown that precipitation tendencies estimated by the least squares method for Russia and Far East in the 20th century and second half of the century are unstable and insignificant (Rankova and Gruza, 1998; Dashko *et al*., 1997). Precipitation decrease in Japan from 1948 to 1985 (Matsumoto and Yanagimachi, 1991) was not also confirmed later by using extended dataset for the next decade (Tase and Nakagawa, 1990), and confidence probability of trend in precipitation is not high in comparison with that in the air temperature trend.

At the same time, distribution function of precipitation time series is usually abnormal, unlike the distribution function of the air temperature samples. Therefore, in case of precipitation it is more accurate to use the nonparametric robust method for estimation of trend and its statistical significance (Gan, 1995; Krokhin, 1997, 2001). The aim of our study is to estimate centennial/semi-centennial climatic tendencies in the monthly mean surface air temperature and precipitation over Northeast Asia in the 20th century, as well as the trend in the Northwest Pacific SST for the second half of the century. Moreover, dominating low frequency variability of the surface air temperature and precipitation in the Northeast Asia is estimated for the 20th century using wavelet techniques.

OBSERVATION DATA AND STATISTICAL METHODS

The linear trends of surface air temperature and precipitation in the 20th century and the second half of the century are estimated for each month of a year in the wide continental area of the extratropic Asia east of 55°E, from the Ural Ridge to the coastal areas of the Northwest Pacific and Alaska Peninsula. Semi-centennial tendency in the monthly mean SST in the Northwest Pacific region extended to the west of 180°E is examined for the second half of the 20th century. Dataset of monthly mean grid SST also covers East China, Japan, Okhotsk and Bering Seas. Thus, the climate change in the wide latitude band from the North Tropic to the coast of Arctic Ocean is estimated. Monthly mean time series of air temperature and precipitation at the meteorological stations were selected for the area studied from data bases of NOAA Global History Climatic Network (USA), RIHMI-WDC (Russia) and JMA (Japan) for the period of instrumental observations since late 19th century to 2000. To outline the details of climate change associated with extreme cooling or warming in winter and summer, we also used the daily time series of surface air temperature at some meteorological stations. Two monthly datasets of the Northwest Pacific SST on different grids were selected from: (1) WMU/COADS World Atlas of Surface Marine Data NOAA/NESDIS/NCDC CD-ROM, 1994 of time series since 1945 to 1989 with horizontal resolution 1×1°; (2) JMA data base of time series since 1946 to 2000 with horizontal resolution 2×2° for the ocean area 15–65°N, 110–180°E. Initial time series of air temperature, precipitation and JMA SST have missing data. To use complete datasets, missing data of the time series in each month were recovered by the statistical method of incomplete multivariate data analysis (Schafer, 1997) using EM and AM algorithms.

Two methods of the linear trend estimation are applied. The first one is based on the least square (LS) method, Pirson's regression and the Fisher's test for statistical significance level. The second one is the nonparametric robust (NR) method (Holander and Wolfe, 1973; Hettmansperger, 1984), based on Theil's rank regression and the Kendall's test for statistical significance level (Bendat and Piersol, 1986). The NR method should be applied to time series with abnormal distribution function typical mainly for precipitation time series. It does not demand the assumption that function of distribution is Gaussian. In this case the rank statistics is used to determine both linear regression and its significance. The NR method was earlier applied to examine trends of precipitation in Canada and northeastern USA (Gan, 1995), as well as, in Russian Far East for a warm season (Krokhin, 1997, 2001). To estimate trends of surface air temperature, precipitation and SST we have applied both LS and NR methods to all time series independently on distribution function of datasets.

We also use wavelet techniques (Grossman, 1988) to reveal seasonality of dominating climate oscillation in monthly surface air temperature and precipitation over Northeast Asia. The method and its possible applications in physics are explained in details by Astafieva (1996). Application of wavelet analysis in geophysics, meteorology and oceanography is also explained in (Salomatin *et al.*, 2000). Using MATHLAB software and "sombrero" wavelet, we estimate the amplitude and phase of climate oscillation of ENSO, decadal and interdecadal time scales.

CLIMATIC TENDENCY IN SURFACE AIR TEMPERATURE

Large-scale areas of warming and cooling in the Northeast Asia and their seasonality are revealed for both the whole period of instrumental meteorological observations and the second half of the 20th century by using two statistical methods of linear trend estimation. The sign and confidence probability of semi-centennial air temperature trend for the second half of the 20th century are shown in Figure 1 for winter and summer months. The area studied is mostly covered by observation data for this period.

A semi-centennial warming (0.02°C/year) of high confidence probability of 99% (Figure 1) in the second half of the 20th century is clearly recorded over subtropic Pacific marginal zone (Korean Peninsula, Japanese Islands) all the year round, over Kamchatka Peninsula in summer, spring, and fall, and at the Pacific side of Alaska Peninsula in most months. Weak semi-centennial warming is also found over Chukotka Peninsula, but only in summer months. Significant semi-centennial cooling (from 1946 to 2000) in the Northwest Pacific marginal area is found in southeast subtropic continental area adjacent to the East China Sea in the latitude band of 25–35°N (Figure 1a, c, d). Negative air temperature trend with confidence probability of 95–99% occurs in the latitude band of 25–35°N in June and July (-0.04°C/year), and in 25–30°N band it occurs in August, September (-0.02°C/year), October, December, March and April (-0.01°C/year). Significant centennial cooling in other months is also typical for this latitude band but mainly in the offshore continental area. The most substantial seasonality of semi-centennial air temperature trends is found in the continental area of 35–55°N, 90–110°E. As shown in Figure 1, seasonality of climatic trend in this large-scale area is characterized by warming in winter and cooling in summer. Positive temperature trend in this area is the most significant and expanded in December–March, whereas negative one expands in June–September with maximum significance in June–July. Correspondingly, differences between monthly mean air temperature in June and December, July and January, August and February substantially decrease in this continental area both in the 20th century and the second half of the century. Substantial difference of the air temperature tendencies in the offshore continental area and marginal zone of the Northwest Pacific is also manifested. It seems to be due to amplification of ocean impact to the mid-latitude Asian continental areas, as well as to long-term anomaly of the Asian monsoon system.

Statistically significant centennial warming (0.03°C/year) from the beginning of the 20th century till 1990 or 2000 also occurs over the marginal subtropic Northwest Pacific throughout a year, over subarctic coastal area in most months, and over arctic

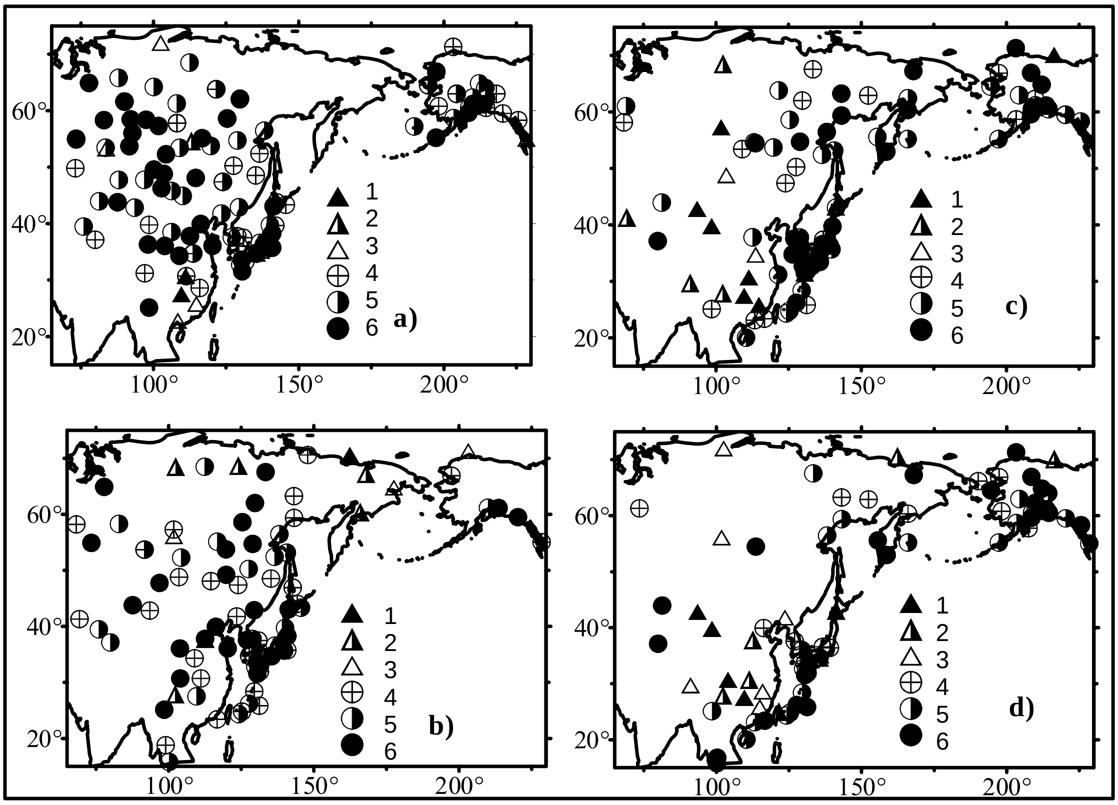

Figure 1. Negative (1, 2, 3) and positive (4, 5, 6) tendencies of surface air temperature with confidence probability: 90% (3, 4), 95% (2, 5) and 99% (1, 6) in December (a), January (b), June (c), and July (d) for the time series since 1945 till 2000

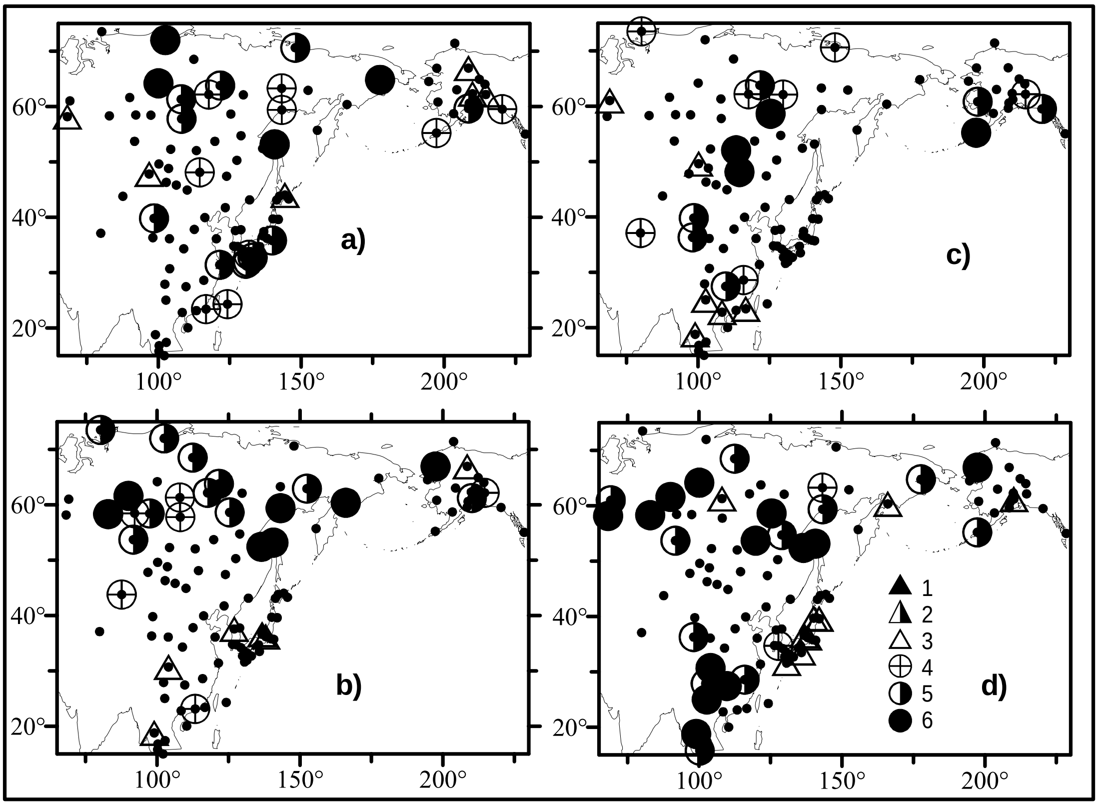

Figure 2. Negative (1, 2, 3) and positive (4, 5, 6) tendencies of precipitation sum with confidence probability: 90% (3, 4), 95% (2, 5) and 99% (1, 6) in March (a), October (b), June (c), and January (d) for the time series since 1945 till 2000

marginal zone only in a few months, particularly, in December, January, July and August. Centennial trend in offshore area of mid-latitude continental Asia also shows warming in winter and cooling in summer (Ponomarev *et al.*, 2001). So, centennial and semi-centennial trends of surface air temperature are similar and stable. At least, at the meteorological stations where the period of instrumental observations is more than 100 years (Japan, Korea, Russia), sign and significance of centennial trend do not substantially depend on a period of time series varying from 73 to 120 years. Similar patterns of linear trends in the area studied were found for the datasets of monthly mean air temperature since beginning of instrumental observations in late 19th century until 1990 or since 1917 until 1990 (Ponomarev *et al.*, 2001). It is also in agreement with tendencies of annual/seasonal mean surface air temperature and other climatic characteristics estimated for different countries, including Japan, Russia, China, Korea and so on (Arakawa, 1957; Rankova and Gruza, 1998; Varlamov *et al.*, 1998; Tyson *et al.*, 2002). On the whole, significant warming of both centennial and semi-centennial scale predominates in a cold period of a year in a broad mid-latitude continental zone north of 35–40°N (Figure 1a).

CLIMATIC TENDENCY IN PRECIPITATION

Statistically significant (with 95–99% confidence probability) trends of precipitation for the second half of the 20th century (1945–2000), as well as for the 20th century (1900–2000; 1916–2000) are revealed in large-scale areas of the Northeast Asia for each month of a year. This result is not in agreement with conclusion on statistical non-significance of precipitation trends estimated earlier by traditional least squares (LS) method in (Dashko *et al.*, 1997; Rankova and Gruza, 1998). A sign and confidence probability of semi-centennial trend of monthly precipitation estimated in by the nonparametric robust (NR) method are shown in Figure 2 (p. 127).

Increase of precipitation in the second half of the 20th century is found in large-scale continental areas of the Northeast Asia prevailing in October–May in the moderate and arctic latitude zones. Typical monthly precipitation rise of high confidence probability (99%) is 0.2–0.4 mm/year, and maximum values are in the range of 1.4–1.7 mm/year at some Russian meteorological stations in the continental area of the moderate latitudes. In October–February the positive semi-centennial trend of monthly precipitation sum occurs east of 55°E in the whole latitude band of 45–70°N, but in March, May and June it occurs in the area east of 100°E in the same latitude band. In February the positive precipitation trend of high confidence probability (99%) also occurs in the tropical and subtropical marginal area east of 95–100°E adjacent to the East China Sea, where the air temperature trend is also positive. Negative precipitation trend (0.1–0.2 mm/year) in this subtropical area is found in May and October, and only at some meteorological stations it takes place from July to September. Bands of positive precipitation trend in summer months are stretched out from southwest to northeast, parallel to the Northwest Pacific marginal zone (Figure 2c). In June positive precipitation trend (0.2–0.5 mm/year) occupies the area along the Pacific and Bering Sea coast of Alaska and offshore band stretching out from continental area adjacent to the East China Sea to the arctic coast of the East Siberian Sea. So, positive patterns of precipitation and air temperature trends are very similar in the continental area of the Northeast Asia. Warming accompanies precipitation rise there. This result is close to conclusion on the accompanying centennial trends of global/hemisphere means air temperature and precipitations (Bradley *et al.*, 1986; Vinnikov *et al.*, 1990; Kondratiev and Demirchan, 2001; and others). Weak negative trend of precipitation is found in Japan south of Hokkaido and in Russian Primorye region adjacent to the Northwest Japan Sea. In this area of the NW Pacific marginal zone centennial and semi-centennial warming accompanies precipitation decrease. Relatively weak (with confidence probability of 90–94.9%) negative precipitation trends of both centennial and semi-centennial (Figure 2c, d) scales are found over Kyushu and Honshu Islands in September, October, December and January. Similar trends with low confidence probability (<90%) are found in Russian Primorye region in most months (Krokhin, 2001).

Significant positive precipitation trend occurs in Kyushu and Honshu Islands: centennial trend in May, and semi-centennial in March (Figure 2a). In the subarctic zone (Hokkaido, Sapporo) centennial increase of precipitation with high confidence probability (95–99%) occurs in January, February, March and August, and decrease of precipitation occurs in May, June, and July. Thus, seasonality of precipitation trend over Japanese Islands is significant and shows opposite patterns of trend in subtropic and subarctic zones. It is also controlled by storm track change like in low frequency anomalies (Branstator, 1995), including extratropic ENSO signal (Chan, 1985) and decadal oscillation (Nakamura *et al.*, 1997). In case of precipitation trends estimated by the Nonparametric Robust (NR) method are more objective and have greater reliability than LS method. About 50% of precipitation time series even for the whole period of instrumental observation have abnormal distribution function usually with substantial positive skewness and an abnormal kurtosis. Substantial difference for this case between statistical significance of the centennial precipitation trends in Japan estimated by NR and LS methods is demonstrated in Table 1 and Figure 3.

Table 1

Increment (Inc.) and confidence probability (CP) of precipitation trend in October estimated by LS and NR methods for some time series at Japanese meteorological stations since 1900 till 1998 (1) and since 1916 till 2000 (2) with abnormal skewness and kurtosis

Stations	Inc. LS (mm/year)		Inc. NR (mm/year)		CP LS, Fisher test (%)		CP NR, Kendal test (%)		Skewness		Kurtosis	
	1	2	1	2	1	2	1	2	1	2	1	2
Akita	-0.4	-0.6	-0.3	-0.6	89.4	96.9	92.7	99.3	0.6	0.3	1.3	0.2
Miyako	-0.8	-1.0	-0.8	-1.1	98.0	98.4	99.4	99.8	1.0	0.8	0.9	0.2
Osaka	-0.3	-0.4	-0.4	-0.4	87.6	83.2	97.9	92.4	0.8	0.9	0.4	0.4
Shionomisaki	–	-1.3	–	-1.2	–	96.6	–	97.6	–	0.9	–	0.5
Choshi	–	-1.0	–	-1.2	–	95.3	–	99.7	–	1.2	–	3.1
Kanazawa	–	-0.8	–	-0.6	–	96.3	–	98.6	–	1.4	–	3.2
Kagoshima	-0.5	-0.2	-0.7	-0.3	90.4	44.6	99.7	90.7	1.3	1.6	2.1	2.9
Matsumoto	-0.3	-0.6	-0.3	-0.5	83.3	95.3	95.5	98.0	1.9	2.1	6.6	7.2
Miyazaki	–	-1.2	–	-0.7	–	86.2	–	95.3	–	2.1	–	4.5

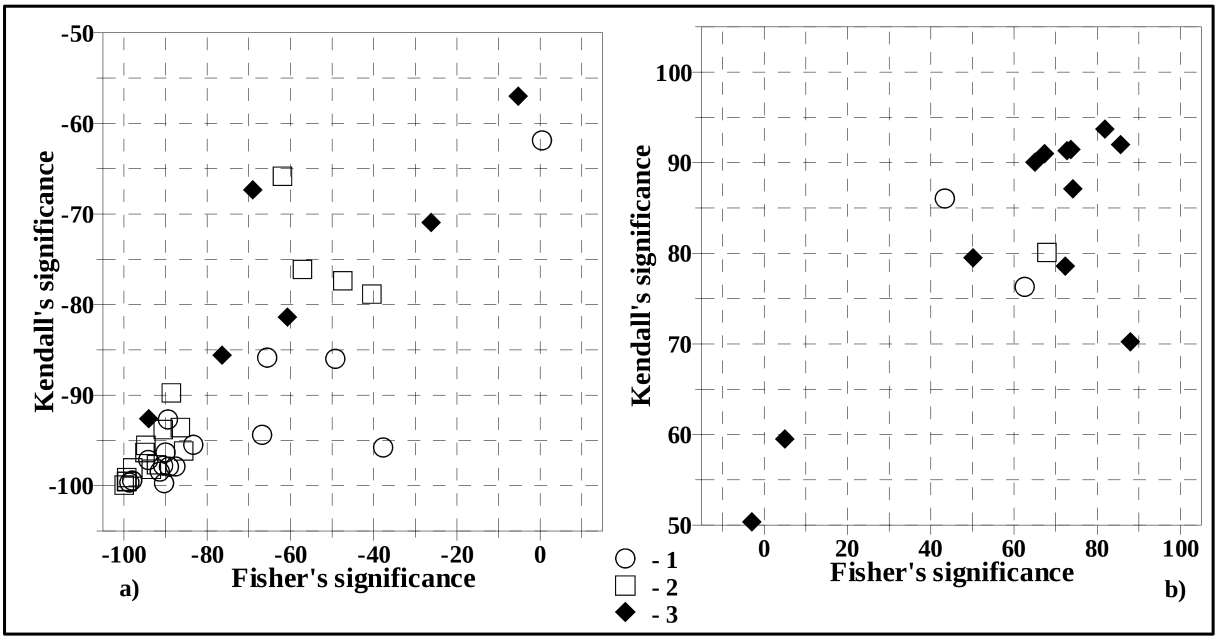

Figure 3. Confidence probability (%) of negative (a) and positive (b) centennial (1900–2000) trends of monthly precipitation in Japan for October (1), December (2), and May (3) estimated by LS method with Fisher's test and by NR method with Kendal's test for significance level. A negative value of in axis (a) means negative trend

The trends in precipitation estimated by both methods for the centennial time series in Honshu and Kyushu Islands are negative in October. It is shown in Table 1 and Figure 3 that confidence probability (CP) of precipitation trend estimated by NR method is higher than CP estimated by LS method in all cases with abnormal distribution functions for both time series: since 1900 until 1998 (1) and since 1916 until 2000 (2). Increment of the trend does not significantly depend on the method applied, and it depends more on the time period examined. Increment of the trend for the period 1916–2000 is higher than for the period 1900–1998.

Thus, the difference and similarity between the trend and its significance estimated by two methods substantially depend on the distribution function, and mainly, on its skewness. NR method allows to get the most stable estimation of climatic trend in case of precipitation.

CLIMATIC TENDENCY IN THE NORTHWEST PACIFIC SST

The trend of annual mean SST of the World Ocean in 5° longitude-latitude bins was earlier analyzed by Casey and Cornillon (2001) for the period 1942–1993. In comparison with (Casey and Cornillon, 2001) we revealed regional details of high seasonality in SST tendency in the Northwest (NW) Pacific for the second half of the 20th century (1945–2000), estimating linear trend in a grid 2×2° for each month

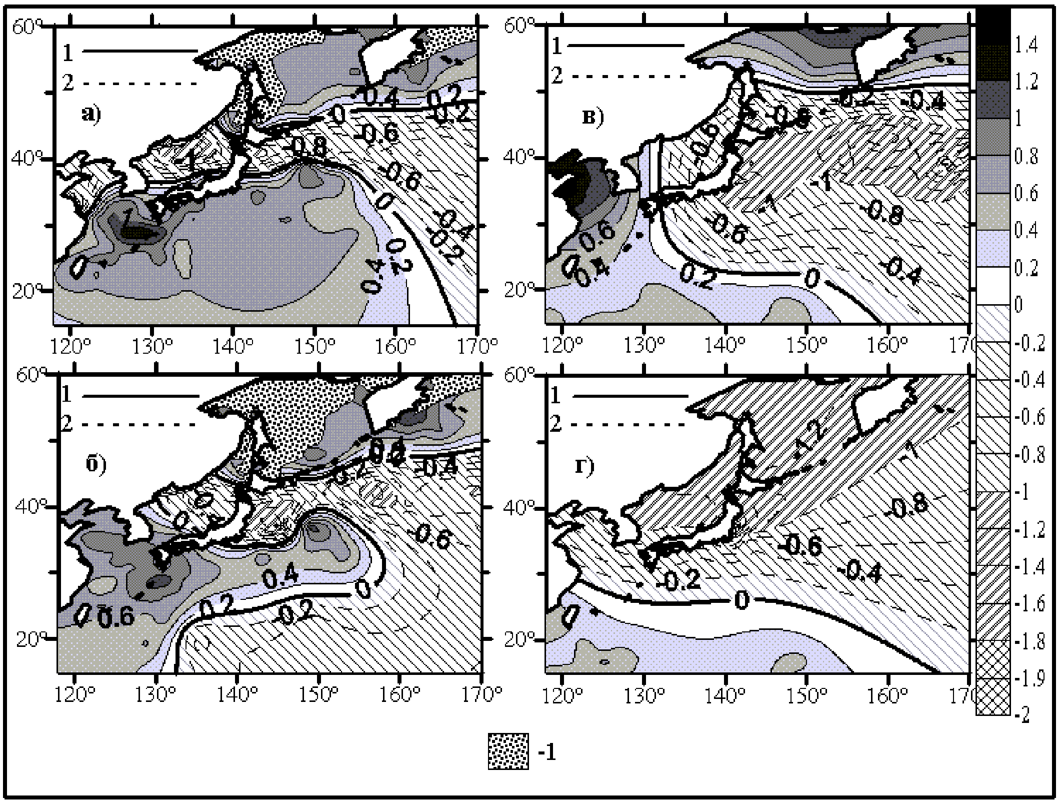

Figure 4. Positive (curve 1) and negative (curve 2) increment (°C) of linear trend in SST (JMA) since 1946 until 2000 in January (a), February (b), July (c), and August (d). Ice coverage in marginal seas is filled by special pattern

of a year. The SST trends for two months of both winter and summer seasons are shown in Figure 4 demonstrating high seasonality.

Seasonality of SST trend is similar to that of surface air temperature trend over the Northeast Asia (Figure 1). Semi-centennial warming in SST dominates in November–January (Figure 4a), and cooling dominates in July–September (Figure 4c). It is important that warming tendency in November–December takes place, at first, in the western tropic and subtropic area including west Philippine Sea, East China Sea, Kuroshio region, and at second, it occurs in the northwestern subarctic Pacific. Warming in the cores of both pools is most significant (99%) and highest (0.8–1.3°C per 55 years) in December. The subarctic pool of warming in December occupies offshore Oyashio region, as well as areas adjacent to western Aleutian Islands and Kamchatka Peninsula. The most significant positive trend in the Northwest Pacific SST occupies indeed the largest area in December. In January subtropical warming pool expands northeastward to Kuroshio Extension and transition zone south of subarctic front (Figure 4a). In January–February the subarctic pool of warming also shifts northeastward to the southwest Bering Sea and ocean area adjacent to the north Kamchatka (Figure 4a, b).

At the same time, in January significant trend of cooling occurs in the latitude band of 39–45°N east of Tsugaru Strait and Hokkaido Island, extending eastward. This area of long-term cooling is associated with Oyashio, its intrusion and subarctic frontal zone. In February the pool of cooling occupies most of the western subarctic gyre, dominating in the Oyashio Intrusion and western core of the subarctic gyre. In March–May it expands substantially southward, occupying northeast area of the subtropic gyre. Pool of cooling also expands in subarctic gyre in spring, becomes deepest in July, and occupies NW Pacific north of 30°N in August with maximum negative SST trend in the Japan and Okhotsk Seas, being weak and insignificant in subtropical area and transitional zone.

Features of both SST trends and circulation change in the Japan Sea are very close to that in the Northwest Pacific. Warming in winter SST occurs in south subtropic region adjacent to Korean Strait and north subarctic area adjacent to Tatarskiy Strait, but the cooling pool occupies the central sea area associated with the subarctic gyre and subarctic frontal zone where intermediate low salinity water forms through the subduction mechanism in late fall and winter. Subtropic gyre in the Japan Sea spins up in the late 20th century, which follows from observation data analyses and modeling results presented in (Trusenkova *et al*., 2003). Anomalously increased heat transport from the western subtropic Pacific and East China Sea to the Japan Sea accumulates in its intermediate and deep waters (Ponomarev and Salyuk, 1997; Ponomarev *et al*., 2000a, 2001), but semi-centennial trend in SST of subarctic gyre is negative. Physical mechanism of the SST cooling in the southwest area of the Northwest Pacific subarctic gyre, accompanying warming in the Kuroshio and Aleutian current systems seems to be similar to anatomy of climate change in the main pycnocline of the Japan Sea.

SEASONALITY OF LOW FREQUENCY CLIMATE OSCILLATION

Significant centennial regional climatic tendencies over the North Hemisphere Asian Pacific region in the 20th century may be caused both by anthropogenic factors and the natural secular oscillation with the period of a couple of centuries (Arakawa, 1957; Israel *et al*., 2001). High regional semi-centennial winter warming in the Northeast Asia and subtropic Northwest Pacific in the second half of the 20th century can also depend on the warm phase of a 30–50 year period variation. A 50–70 year climatic oscillation over the North Pacific and North America are revealed in the winter–spring Sea Level Pressure (SLP) and the spring–summer SST (Minobe, 1997). The 50 year climate oscillations are examined by Minobe (1997) on the base of the Multi-Taper-Method applied to the analysis of the meteorological observation data over the North Pacific, North America and tropical ocean until 1990, as well as the reconstructed climate records of the surface air temperature for the North America from the tree-ring data since the 17th century.

We would compare seasonal features of the dominating oscillations in the surface air temperature and precipitation over the Northeast Asia with the seasonality of centennial/semi-centennial trends in the Northeast Asia and Northwest Pacific. Based on the wavelet technique (explained in details by Grossman (1988), Astafieva (1996), and Salomatin (2000)) we analyzed the time series of the monthly mean surface air temperature and precipitation only at the meteorological stations in the Northeast Asia for the period of instrumental observations including the time series since 1916 until 2000. Similar to trend analysis we consider, at first, the original time series at the basic meteorological stations with the minimum missing data. The time series are relatively short for the wavelet transform. Therefore, the units in a sample for the time series are artificially increased by the spline approximation. A "sombrero" wavelet in the MATHLAB software is used to damp the biennial oscillation. In this case, wavelet transforms show the evolution of frequency, amplitude and phase of the dominating climate oscillation of the ENSO (3–7 years), decadal (8–13), and interdecadal (18–30 years) time scales. When the "sombrero" wavelet is used, the anomalies of 35–40 years associated with the estimated trend are detected.

Typical wavelet transforms of the surface air temperature in January (a, c, e, g) and August (b, d, f, h) at four meteorological stations situated in different climatic zones of the offshore continental area of moderate latitudes (Irkutsk 52.27°N, 104.32°E), as well as in the arctic transitional zone (Anadyr 64.78°N, 177.57°E) and subarctic region (Okhotsk 59.37°N, 143.2°E and Petropavlovsk-Kamchatskiy 52.98°N, 158.65°E) of the Northwest Pacific marginal area are presented in Figure 5. Only positive temperature anomalies of different time scale alternated with the periods from 3 to 42 years (axis of ordinates) are outlined by the shade of black and grey in this figure. Negative anomalies filled by white are invisible in the figure. Similar wavelet transforms of precipitation time series are shown in Figure 6 with exception of (g) and (h). The positive anomalies of precipitation in Vladivostok are demonstrated in Figure 6g, h.

The alternation of the positive temperature and precipitation anomalies related to the ENSO scale oscillation (3–7 years) is presented in the top part of Figures 5, 6. It is one of the prevailing oscillations both in subtropic (Hanawa *et al*., 1988, 1989; Wang *et al*., 1999) and subarctic regions of the Northwest Pacific (Oh and Park, 1999; Ponomarev *et al*., 1999a, 1999b, 2002), its marginal seas and adjacent land area of the Northeast Asia (Fu and Teng, 1993; Volkov *et al*., 1997; Ponomarev *et al*., 1999a, 1999b, 2002; Oh and Park, 1999). Variability of ENSO scale in the area studied is associated with the unlagged and lagged extratropic El Niño/La Niña signals interacting with the internally generated oscillations due to the nonlinear atmosphere-ocean dynamics.

Winter El Niño accompanies the warming in the subtropic Northwest Pacific and the adjacent land, and the cooling in the subarctic ocean/land area during winter at a high confidence probability. The winter La Niña accompanies the cooling in the subtropics and the warming in the subarctic marginal area during winter, also at a high confidence probability. Similar winter anomalies occur after the preceding summer La Niña events, while the warming/cooling in summer is typical after the winter La Niña/El Niño both in subtropic and subarctic land and ocean areas (Ponomarev *et al*., 1999a, 1999b, 2002). Coefficients of the cross-correlation between the SOI and the winter mean surface air temperature at the meteorological stations around the Sea of Okhotsk are shown in Table 2. The low-frequency thermal regime variations also manifest themselves in the Okhotsk Sea ice. Sea ice winter mean time series (1957–1989) were composed by averaging the 10-day ice cover in winter and early spring (21–28 of February, 1–10, 11–20 and 21–30 of March, and 1–10 of April). Both its unlagged and lagged (ice 6-month lagging SOI) cross-correlation with SOI is statistically significant and negative (Table 3). Thus, the ice cover in the Okhotsk Sea tends to increase during the winter El Niño events (when SOI reaches its highest negative values) and to decrease in the winters following the summer La Niña events (when SOI reaches its highest positive values).

Table 2

Cross-correlation of winter mean air temperature time series (1949–1990) at the coastal meteorological stations around the Sea of Okhotsk with each other and SOI averaged for the same winter, next summer (SOI, +6 m.) and previous summer (SOI, -6 m.)

	Okhotsk	Ajan	Icha	Niko-laevsk	Alexan-drovsk	Poro-naysk	Aba-shiry	Nemu ro	SOI	SOI, +6 m.	SOI, -6 m.
Magadan	0.93	0.53	0.79	0.42	0.43	0.52	none	none	0.54	none	0.43
Okhotsk		0.66	0.71	0.58	0.52	0.59	none	none	0.58	none	0.38
Ajan			0.48	0.68	0.78	0.69	0.4	0.47	0.41	none	none
Icha				0.46	0.57	0.59	0.46	0.47	0.51	none	0.42
Nikolaevsk					0.73	0.66	0.50	0.52	0.38	none	0.32
Alexandrovsk						0.84	0.71	0.75	0.42	none	0.28
Poronaysk							0.49	0.57	0.56	none	0.43
Abashiry								0.97	none	none	none
Nemuro									none	none	none

Note:

Linear trend is subtracted.

95%-confidence level is equal to 0.308, according to the Fisher test.

Table 3

Unlagged and lagged cross-correlation with SOI of some oceanographic and meteorological characteristics in the Sea of Okhotsk calculated for the winter mean time series

Data	Unlagged SOI	SOI 6 months leading	95%-level
Ust-Hairuzovo air temperature, 1950–1990	0.55	0.34	0.312
Okhotsk sea ice, 1957–1990	-0.45	-0.46	0.349
North Pacific Index, 1940–1990	0.58	0.49	0.282

Note:

95%-confidence levels are calculated using the Fisher test

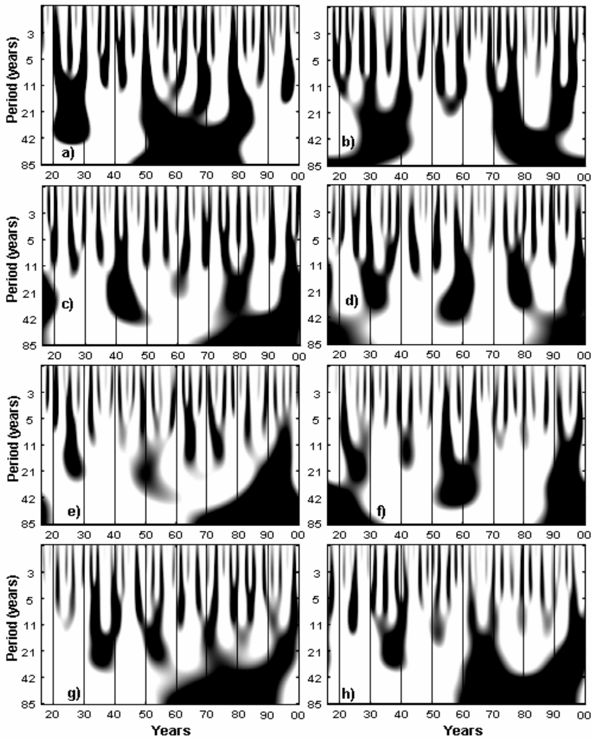

Figure 5. Wavelet transform of monthly mean surface air temperature in Anadyr (a, b), Okhotsk (c, d), Irkutsk (e, f), and Petropavlovsk-Kamchatskiy (g, h) for January (a, c, e, g) and August (b, d, f, h) since 1916 until 2000 year (abscissa axis)

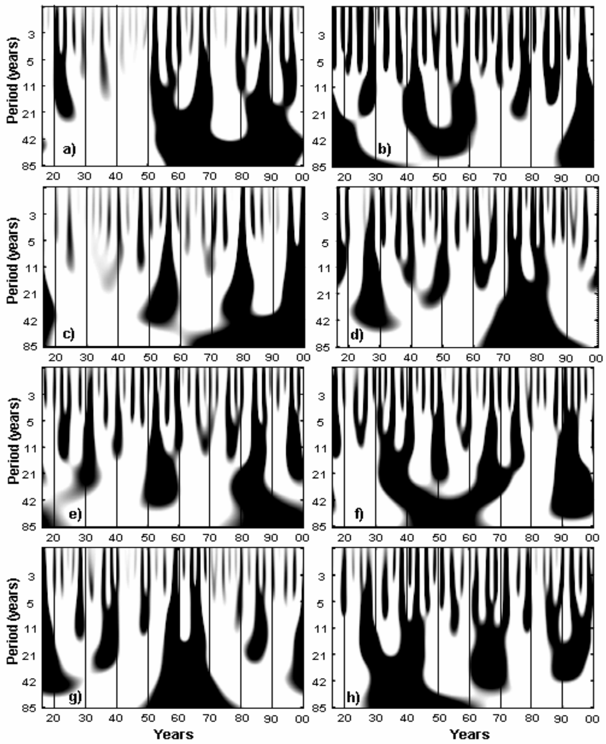

Figure 6. Wavelet transform of monthly precipitation sum in Anadyr (a, b), Okhotsk (c, d), Irkutsk (e, f), and Vladivostok (g, h) for January (a, c, e, g) and August (b, d, f, h) since 1916 until 2000 year (abscissa axis)

Unlagged monthly ENSO-scale anomalies in the extratropic Asian Pacific are due to El Niño/La Niña-accompanying anomalous circulation processes in the extratropic atmosphere and ocean. The relationship between heat displacement during ENSO cycle in tropics and the intensity of trade winds (Wyrtki, 1975), location and intensity of the atmospheric circulation patterns (Horel and Wallace, 1981) and centers of action in the Asian Pacific, as well as Hadley circulation and westerly jet stream (Lau and Boyle, 1987; Yang and Webster, 1990; Oort and Yienger, 1996), South Asian, Indian and East Asian monsoons (Wu and Hastenrath, 1986; Webster and Yang, 1992; Tyson *et al.*, 2002) are actually considered as important physical devices of tropic-extratropic interaction, and the extratropic response to ENSO in the atmosphere. According to Sekine (1996), at least, La Niña event is effected by the anomaly of the winter snow coverage over the Asian continent and the summer monsoon wind. In this case the low frequency anomalies of the Northeast Asia monsoon system also have an impact on the anomalies of the tropical ENSO cycle.

Lagged and unlagged ENSO-scale remote linkages are actualized through the synoptic scale physical processes both in the atmosphere and ocean with the propagation of the faster, barotropic (Simmons *et al.*, 1983) and slower, baroclinic (Lau and Boyle, 1987) waves in the atmosphere, coastal Kelvin and Rossby waves in the North Pacific Ocean (Johnson and O'Brien, 1990), as well as the coupled atmospheric-oceanic waves in the global ocean-atmosphere (White and Cayan, 2000). The ENSO-scale variability in the Asian Pacific region is also considered as a response to the huge heat displacement in the tropics accompanying substantial seasonal anomalies in the tropical cyclone activity (Chan, 1985, Chen and Weng, 1998) in the Western Pacific and extratropical storm tracks change (Branstator, 1995). As for oceanic teleconnections, the poleward ENSO signal propagation in the North Pacific is explained by Johnson and O'Brien (1990). By the circulation model and observation data analysis, they show that the temperature and upper layer thickness anomalies propagate northward along the eastern coast of the North America due to the coastal Kelvin waves, and reach the 50°N latitude in about one year. Further in mid-latitude the westward temperature anomaly propagation to the central mid-latitude Pacific is due to the baroclinic Rossby waves excited by the coastal Kelvin waves. Formation of the temperature anomaly in the central Pacific accompanies the circulation change in the atmosphere and the North Pacific Ocean. Thus, one can suggest that both a northward fast ENSO signal in the atmosphere and a slow ENSO signal in the ocean exist. Propagation of both signals is controlled by synoptic-scale processes, atmospheric ones of an order of a week, and oceanic ones of an order of a few months, which, in turn, interact with the larger-scale processes.

A lot of meteorological and oceanographic data observed in tropics and extratropics during ENSO events were collected and analyzed particularly on the base of the TOGA project. As suggested, the irregularity of ENSO may be caused by the nonlinearity in the ocean-atmosphere system, particularly, by the nonlinear interactions between the heat displacement in tropics and the anomalies of annual cycle in the extratropics. At the same time, substantial anomalies of ENSO cycles and changes of El Niño and La Niña occurrence during the winters from 1950 to 1995 are shown by Zhang and Wallace (1996) and others. In particular, the La Niña occurrence in winter dramatically decreased since 1977. After the maximum interval between El Niño events from 1974 to 1982, La Niña events have become weaker and have taken place mostly in summer while El Niño have been dominating in winter, have become more frequent since 1987, and especially in 1990s.

The ENSO-like interdecadal variability is shown by Wang (1995) and Zhang *et al.* (1997), and interdecadal variability in the western Pacific and its amplification in global warming is manifested by Yamagata and Masumoto (1992). At the same time, the positive SST trend dominating during winter in the subtropic NW Pacific and the negative SST trend prevailing during summer in the subarctic NW Pacific (Figure 4) also look like accumulated El Niño impact. On a whole, the seasonality and regionality of the positive/negative anomalies of the El Niño signal in the extratropic Northwest Pacific are similar to the seasonality and regionality of positive/negative climatic trends in this large-scale area of the North Pacific (Figure 3). The questions arising from our study are why the anomalies of so different scales have a substantial similarity in the NW Pacific, and what forcing drives climate in the 20th century?

The alternation of positive/negative temperature anomalies with decadal (8–13) and interdecadal (18–30 years) time scales is shown in the mid part of Figures 5, 6. Similar oscillations of both scales were studied through the observation data analysis for the Northern Hemisphere (Trenberth, 1990) and the Pacific ocean-atmosphere system (Trenberth and Hurrel, 1994; Chen and Ghil, 1995; Yasuda and Hanawa, 1997; Nakamura *et al.*, 1997; Minobe and Mantua, 1999; Miller and Schneider, 2000; Tourre *et al.*, 2001), as well as by simulation with the circulation models of the North Pacific Ocean (Latif and Barnett, 1994; Miller *et al.*, 1994; Schneider *et al.*, 2002; Auad, 2003; Qiu, 2003), and the simulation with the coupled model showing a 30-year interdecadal mode (Robertson, 1996), also found in the Global Sea Ice Coverage and SST data set (Auad, 2003). Main features of decadal-interdecadal dynamics associated with the low frequency variations of the Aleutian Low, wind stress curl, subduction in the central NW Pacific, SST anomaly in the Kuroshio-

Oyashio Extension area, as well as positive feedback from the SST anomaly to the Aleutian Low are described in (Miller and Schneider, 2000; Schneider *et al*., 2002).

By the data analysis, Tourre *et al*. (2001) found that the oscillations of decadal (8–13) and interdecadal (longer than 13 years) time scales are quite different and statistically independent. The substantial differences between the decadal (8–13) and interdecadal (18–26 years, bi-decadal scale) bands in the North Pacific Ocean were shown and explained by Auad (2003) based on numerical experiments with the isopycnal ocean model forced by the NCEP-NCAR reanalysis wind stress and heat fluxes for the period since 1958 until 1997. According to the simulation results, the decadal band is mostly driven by the wind stress curl, unlike the interdecadal band, which is mostly driven by the atmospheric heat fluxes exciting a high baroclinic mode and counterclockwise pycnocline anomaly moving around the basin (Auad, 2003). This pycnocline anomaly of interdecadal time scale moves across the Gulf of Alaska toward the Aleutian Island up to about Kamchatka Peninsula, continuing to the southwest down to about 28°N. Auad (2003) has also shown that the maximum SST variability takes place west of the date line at 45°N and along the eastern boundary in the interdecadal band and in the central North Pacific and Kuroshio-Oyashio Extension areas in the decadal band. According to Qiu (2003), the Kuroshio Extension jet is weakening and strengthening with a prevailing period of about 12 years that is caused by the wind stress curl anomalies.

At the same time, the SST anomaly of joint ENSO-decadal band can also propagate from the Aleutian Low area to the central region of the subarctic gyre, as well as from the Kuroshio-Oyashio Extension and central subtropic Pacific areas to the western tropical region (Ponomarev *et al*., 1999b; 2000b). The frequency of the SST anomalies can drift in some areas from ENSO to decadal scale within the observational records.

The decadal and interdecadal variability in terms of the wavelet transforms of the air temperature and precipitation in some regions of the Northeast Asia are shown in the mid parts of Figures 5, 6. The bi-decadal (18–26 years) oscillation both in the air temperature and precipitation is indeed most evident in the subarctic marginal Northwest Pacific zone, particularly, in the Kamchatka Peninsula and Okhotsk Sea area: Petropavlovsk-Kamchatski (Figure 5g, h), Okhotsk (Figure 5c, d). The decadal (8–13 years) oscillations are most evident in the arctic marginal zone, including western Bering Sea (Figure 5a, b; Figure 6a, b) all the year round, as well as over land in the latitude band of Kuroshio-Oyashio Extension area mainly in months of the cold period of a year. The period of interdecadal variability in most of these regions shifts to the red spectrum and comes to about a 30–40 years band (Figure 5e, f; Figure 6e, f). In a transitional zone between the subarctic and subtropic regions, continental and marginal areas of the Northeast Asia the frequency of the prevailing variability in the joint decadal-interdecadal band is drifting from the decadal to interdecadal scale up to 30–40 years or from the interdecadal to decadal scale within the period of observations (Figure 5c; Figure 6d, g). It seems to be due to the nonlinear dynamics in the ocean-atmosphere system.

Figures 5, 6 also show seasonality of the positive 20–30 year anomalies associated with the long-term oscillations with a period of 40–60 years (Minobe, 1997). The winter anomalies of this scale both in the air temperature and precipitation in Chukotka Peninsula have an opposite sign in comparison with the summer one. Positive interdecadal anomaly of the air temperature in Anadyr occurs from 1950s to 1970s in January (Figure 5a) and from the late 1970s to early 1990s in August (Figure 5b). It is in agreement with the negative winter temperature trend and the positive summer temperature trend estimated for the second half of the 20th century. In most subarctic area the positive long-term anomaly of the winter air temperature occurs in late 1970s–1990s (Figure 5c, e, d), and the negative anomaly takes place in 1930s–1940s. A positive long-term anomaly of the winter precipitation in the subarctic area is also revealed in late 1970s–early 1990s or in 1980s–1990s for the most subarctic marginal and continental areas (Figure 6c, e). On the contrary, a negative 35–40 year anomaly of the summer precipitation in a subarctic marginal zone (Figure 6d) and the winter precipitation in subtropics are found for the last two decades of the 20th century.

The long-term anomalies are similar and more evident in the wavelet transforms for the air temperature/precipitation time series since the late 19th century until 2003 (not shown in the figures). In this paper we demonstrate only a historical period of the observations, which is the same for the most of the time series analyzed. The boundary artificial effect of the wavelet transforms (Astafieva, 1996; Salomatin, 2000) at the lower left and right edges (bottom left and right edges of Figures 5, 6) is not high. We compared the wavelet transforms for two samples of the air temperature in Vladivostok: 1872–2003 and 1916–2000. The characteristic time-scale of the artificial negative/positive anomaly at the edge does not exceed 5 years for the band with the periods of 30–40 years.

CONCLUSION

Climatic tendencies in the Northeast Asia in the 20th century are characterized by the significant warming in winter and the cooling in summer over the offshore continental area west of 120–110°E in mid and moderate latitudes. Difference between the summer and winter surface air temperature is significantly decreasing in this continental area during the 20th century and its second half. The warming tendency being characteristic throughout a year for the area east of 110–120°E accompanies the precipitation increase in this area of moderate latitudes. Thus, the continental climate in moderate latitudes of the Northeast Asia becomes closer to marine climate. The positive air temperature trend occupies the marginal land area adjacent to the Northwest Pacific practically all the year round, with the exception of the subtropic continental area adjacent to the East China Sea. The warming tendency in fall and winter accompanies the precipitation decrease in Japan and Russian Primorye Region adjacent to the Northwest Japan Sea. Significant precipitation reduction in Japan takes place in October, December and January, with the exception of the subarctic area (Hokkaido Island) where the precipitation slightly increases in December–March and in August, but decreases in May–July.

Statistically significant positive SST trend in the Kuroshio region and in the northwest area of the Pacific subarctic gyre dominates from November to February, accompanying the warming in the continental and marginal areas of the Northeast Asia. The semi-centennial negative SST trend occurs in the Oyashio region and occupies the southwestern area of the subarctic Pacific gyre. As a whole, temperature contrasts between the Asian continent area of moderate latitudes and subarctic Northwest Pacific, as well as the contrast in the SST between the western boundaries and the offshore areas of the Northwest Pacific increases, while the air temperature contrast over the offshore area in the East Asia decreases during the second half of the 20th century. Seasonality of the semi-centennial linear trend in the Northwest Pacific and some areas of the Northeast Asia for the second half of the 20th century is similar to the seasonality of the El Niño signal in the Northwest Pacific SST.

REFERENCES

Arakawa H. **1957**. Climatic change as revealed by the data from the Far East. Weather 12 (2), pp. 46–51.

Astafieva N.M. **1996**. Wavelet analyses: theory and applications. Uspekhi fizicheskikh nauk 166 (11), pp. 1145–1170.

Auad G. **2003**. Interdecadal dynamics of the North Pacific ocean. Journal of Physical Oceanography 33 (12), pp. 2483–2503.

Bendat J.S., **Piersol** A.G. **1986**. Random data: analysis and measurement procedures. New York: John Wiley & Sons Publications, 540 p.

Bradley R.S., Diaz H.F., Eischeid J.K., Jones P.D. Kelly P.M., Goodess C.M., **1986**. Precipitation fluctuations over Northern Hemisphere land areas since the mid-19th century. Science 237, pp. 171–175.

Branstator G.W. **1995**. Organization of stormtrack anomalies by recurring low frequency circulation anomalies. Journal Atmospheric Science, Vol. 52, pp. 207–226.

Casey K.S., **Cornillon** P. **2001**. Global and regional Sea surface temperature trends. Journal of Climate, Vol. 14, pp. 3801–3818.

Chan J.L. **1985**. Tropical cyclone activity in west Pacific in relation to the El Niño-Southern Oscillation phenomenon. Monthly Weather Review, Vol. 113, pp. 599–606.

Chen F., **Ghil** M. **1995**. Interdecadal variability of the thermohaline circulation and high-latitude surface fluxes. Journal of Physical Oceanography 25 (11), pp. 2547–2568.

Chen T.C., **Weng** S.P. **1998**. Interannual variation in the tropical cyclone formation over the western north Pacific. Monthly Weather Review, Vol 126, pp. 1080–1090.

Dashko N.A., Varlamov S.M., Khan E.X., Kim E.S. **1997**. Variability of precipitation above coast of the Japan Sea. Meteorology and hydrology, 12, pp. 12–24.

Folland C.K., Rayner N.A., Brown S.J., Smith T.M., Shen S.S., Parker D.E., Macadam I., Jones P.D., Jones R. N., Nicholls N., Sexton D.M.H. **2001**. Global temperature change and its uncertainties since 1861. Geophysical Research Letters 28 (13), pp. 2621–2624.

Fu C.B., **Teng** H.L. **1993**. Relationship between summer climate in China and the El Niño/Southern Oscillation phenomenon. Frontiers in Atmospheric Sciences, Allerton Press, pp. 166–178.

Gan Th. **1995**. Trends in air temperature and precipitation for Canada and north-eastern USA. Int. Journal Climatology 15 (10), pp. 1115–1134.

Grossman A. **1988**. Wavelet transform and edge detection. Stochastic processes in physics and engineering. New York: Reidel, pp. 149–157.

Hanawa K., Watanabe T., Iwasaka N., Suga T., Toba Y. **1988**. Surface thermal conditions in the Western North Pacific during the ENSO events. Journal Meteorological Society of Japan 66 (3), pp. 445–456.

Hanawa K., Yoshikawa Y., Watanabe T. **1989**. Composite Analyses of wintertime wind stress vector fields with respect to SST anomalies in the Western North Pacific and the ENSO events. Part I: SST composite. Journal Meteorological Society of Japan 67 (3), pp. 385–400.

Hettmansperger Th.P. **1984**. Statistical inference based on ranks. New: John Wilew and Sons Inc. Publications, 334 p.

Holander M., **Wolfe** D. **1973**. Nonparametric statistical methods. New York: John Wilew and Sons Inc. Publications, 407 p.

Horel J.D., **Wallace** J.M. **1981**. Planetary-scale atmospheric phenomena associated with the Southern Oscillation. Monthly Weather Review, Vol. 109, pp. 813–829.

Izrael Yu.A., Gruza G.V., Kattsov V.M., Meleshko V.P. **2001**. Global climate change: the role of anthropogenic impact. Meteorology and hydrology, 12, pp. 12–24.

Johnson M.A., **O'Brien** J.J. **1990**. The Northeast Pacific Ocean response to the 1982–1983 El Niño. Journal Geophysical Research 95 (C5), pp. 7155–7166.

Kondratiev K.Ya., **Demirchan** K.S. **2001**. Earth climate and “Kioto Protocol”. Vestnik Rossiyskoy Akademii Nauk 71 (11), pp. 1002–1009.

Krokhin V.V. **1997**. About some methods of statistical data processing of the monthly sums of precipitation. FERHRI Proceedings. St. Petersburg: Hydrometeorological Press, Vol. 148, pp. 116–127. (In Russian).

Krokhin V.V. **2001**. On the precipitation trends over the Russian Far East in a warm season. Reports of International Workshop on the Global Change Studies in the Far East, Sept. 7–9, 1999. Vladivostok: Dalnauka. TEACOM Publication 7(1), pp. 111–122.

Latif M., **Barnett** T.P. **1994**. Causes of decadal climate variability over the North Pacific and North America. Science 266, pp. 634–637.

Lau K.M., **Boyle** J.S. **1987**. Tropical and extratropical forcing of the large-scale circulation: a diagnostic study. Monthly Weather Review, Vol. 11, pp. 400–428.

Matsumoto J., **Yanagimachi** H. **1991**. Long-term variations of precipitation and snow depth in Japan. Proceedings of Environment Change and Gis. Intern. Symp., Asahikawa, Japan, Aug. 28, 1991, pp. 431–444.

Miller A.J., Cayan D.R., Barnett T.P., Graham N.E., Oberhuber J.M. **1994**. Interdecadal variability of the Pacific Ocean: model response to observed heat flux and wind stress anomalies. Climate Dynamics, Vol. 9, pp. 287–302.

Miller A.J., **Schneider** N. **2000**. Interdecadal climate regime dynamics in the North Pacific Ocean: Theories, observations and ecosystem impacts. Progress in Oceanography, Vol. 47, pp. 355–379.

Minobe S. **1997**. A 50–70 year climatic oscillation over the North Pacific and North America. Geophysical Research Letters, Vol. 24, pp. 683–686.

Minobe S., **Mantua** N. **1999**. Interdecadal modulation of interannual atmospheric and oceanic variability over the North Pacific. Progress in Oceanography, Vol. 43, pp. 163–192.

Nakamura H., Lin G., Yamagata T. **1997**. Decadal climate variability in the North Pacific during the recent decades. Bull. American Meteorological Society 78(10), pp. 2215–2225.

Oh I.S., **Park** W. **1999**. Variability of SST and Atmospheric Variables related to ENSO in the North Pacific and in the East Asian Marginal Seas. Proceedings CREAMS'99 International Symposium, Fukuoka, Japan, 26–28 Jan. 1999, pp. 104–107.

Oort A.H., **Yienger** J.J. **1996**. Observed interannual variability in the Hadley circulation and its connection to ENSO. Journal of Climate 9 (11), pp. 2751–2767.

Ponomarev V., Kaplunenko D., Ishida H. **2001**. Centennial and semi-centennial climatic tendencies in the Asian continental and Pacific marginal areas. Bulletin of Japan Sea Research Institution. Kanazawa University. Japan 32, pp. 77–90.

Ponomarev V.I., **Salyuk** A.N. **1997**. The climate regime shifts and heat accumulation in the Sea of Japan. Proceedings of CREAMS Symposium, Jan. 26–31, 1997. Fukuoka, pp. 157–161.

Ponomarev V.I., Trusenkova O.O., Kaplunenko D.D., Ustinova E.I. **1999a**. Interannual Variations of Oceanographic and Meteorological Characteristics in the Sea of Okhotsk. Proceedings of The Second PICES Workshop on the Okhotsk Sea and Adjacent Areas, 9–12 Nov., 1998, Nemuro, Japan, pp. 31–40.

Ponomarev V.I., Trusenkova O.O., Trousenkov S.T. **2002**. Relationship between surface temperature anomalies in the mid-latitude North Pacific region and ENSO. Reports of the Int. Workshop on Global Change Studies in the Far East, September 7–9, 1999, Vladivostok, Russia, TEACOM Publication 7 (2), pp. 34–65.

Ponomarev V.I., Trusenkova O.O., Trusenkov S.T. **2000**. Propagation of low frequency sea surface temperature anomalies in the North Pacific. Russian Meteorology and Hydrology 6, New York: Allerton Press, Inc., pp. 41–48.

Ponomarev V.I, Trusenkova O.O., Trousenkov S.T., Ustinova E.I., Kaplunenko D.D., Polyakova A.M. **1999**. The ENSO signal in the Northwest Pacific. Proceedings of the Science Board 98 Symposium on the 1997/98 El Niño event, 14–25 Oct., 1998, Fairbanks, PICES Scientific Report 10, pp. 9–31.

Ponomarev V.I., Ustinova E.I., Salyuk A.N., Kaplunenko D.D. **2000**. Climate variation in the Japan Sea and adjacent area in the 20th century. Izvestiya TINRO (Collection of papers Trans. Pacific Res. Fish. Center) 127 (2), pp. 20–36. (In Russian).

Qiu B. **2003**. Kuroshio extension variability and forcing of the Pacific decadal oscillations: responses and potential feedback. Journal of Physical Oceanography 33 (12), pp. 2465–2482.

Rankova E.Ya., **Gruza** G.V. **1998**. Indicators of climate change for Russia. Meteorologiya i Gidrologiya 1, pp. 5–18.

Robertson A.W. **1996**. Interdecadal variability in the multicentury climate integration. Climate Dynamics, Vol. 12, pp. 227–241.

Salomatin A.S., Yusupov V.I., Savelieva N.I., Semiletov I.P. **2000**. Wavelet analyses: examples of processing in acoustic and hydrometeorological data (North Pacific-North Asian region). Hydrometeorological and biochemical research in Arctic. Proceedings of the Arctic Regional Center, Vol. 2, part 1, Vladivostok: Dalnauka, pp. 202–211. (In Russian).

Schafer J.L. **1997**. Analysis of incomplete Multivariate data. London: Chapman & Hall Publications, 430 p.

Schneider N., Miller A.J., Pierce D.W. **2002**. Anatomy of North Pacific decadal variability. Journal of Climate, Vol. 15, pp. 586–605.

Sekine Y. **1996**. Anomalous Oyashio intrusion and its teleconnection with subarctic North Pacific circulation, sea ice of the Okhotsk Sea and air temperature of the Northern Asian continent. Proceedings of PICES Workshop on the Okhotsk Sea and Adjacent Areas, Vladivostok, June 19–24, 1995. Canada, 1996, pp. 177–187.

Simmons A.J., Wallace J.M., Branstator G.W. **1983**. Barotropic wave propagation and instability, and atmospheric teleconnection patterns. Journal Atmospheric Science, Vol. 40, pp. 1363–1392.

Tase N., **Nakagawa** S. **1990**. Spatial and temporal characteristics of precipitation in Japan. Long-term trends of annual precipitation. Annual Report Institution Geosciences Univ. Tsikuba 16, pp. .553–572.

Tourre Y.M., Rajagopalan B., Kushnir Y., Barlow M., White W.B. **2001**. Patterns of coherent decadal and interdecadal climate signals in the Pacific basin during the 20 th century. Geophysical Research Letters, Vol. 28, pp. 2069–2072.

Trenberth K.E. **1990**. Recent observed interdecadal climate change in the Northern Hemisphere. Bull. Amer. Meteor. Society, Vol. 71, pp. 988–993.

Trenberth K.E., **Hurrel** J.W. **1994**. Decadal atmosphere - ocean variations in the Pacific. Climate Dynamics, Vol. 9, pp. 303–319.

Trusenkova O., Ponomarev V., Ishida H. **2003**. Impact of climate change on circulation patterns in the Japan Sea. Journal Hydraulic Coastal Environment Engineering 733/II-63, pp. 131–150.

Tyson P., Fu C., Fuchs R., Lebel L., Mitra A.P., Odada E., Perry J., Steffen W., Virji H. (Eds.) **2002**. Global-regional linkages in the Earth system. Global Change, START, IGBP Series: Springer, 186 p.

Varlamov S.M.,. Kim Y.S, Han E.Kh. **1998**. Recent variations of temperature in East Siberia and in the Russian Far East. Meteorology and hydrology, 1, pp. 19–28.

Vinnikov K.Ya., Groisman P.Ya., Lugina K.M. **1990**. Empirical Data on Contemporary Global Climate Changes (Temperature and Precipitation). Journal of Climate 3(6), pp. 662–677.

Volkov Yu., Kalashnikov B., Zhukov A., Abramich A., Anzhina G. **1997**. Anomalies of the atmospheric processes and possibility of prediction of extreme air temperature in the El Niño year. Trudi DVNIGMI (Collection of papers of the Far East Regional Hydrometeorological Institute) 147, pp. 120–133. (In Russian).

Wang B. **1995**. Interdecadal change in El Niño onset in the last four decades. Journal of Climate, Vol. 8, pp. 267–285.

Wang C., Weisberg R.H., Virmani J.I. **1999**. Western Pacific interannual variability associated with El Niño-Southern Oscillation. Journal Geophysical Research 104 (C3), pp. 5131–5149.

Webster P.J., **Yang** S. **1992**. Monsoon and ENSO: Selectively interactive systems. Quart. J. Roy. Meteorological Society, Vol. 118, pp. 877–926.

White W.B., **Cayan** D.R. **2000**. A global El Niño - Southern Oscillation wave in surface temperature and pressure and its interdecadal modulation from 1900 to 1997. Journal Geophysical Research, 105 (C5), pp. 11232–11242.

Wu M.C., **Hastenrath** S. **1986**. On the interannual variability of the Indian monsoon and the Southern oscillation. Arch. Meteor. Geophys. Biocl., Vol. B39, pp. 239–261.

Wyrtki K. **1975**. El Niño – The dynamic response of the equatorial Pacific Ocean to atmospheric forcing. Journal Physical Oceanography 5, pp. 572–584.

Yamagata T., **Masumoto** Y. **1992**. Interdecadal natural climate variability in the western Pacific and its implications in global warming. Journal Meteorological Society of Japan. Vol. 70, pp. 167–175.

Yang S., **Webster** P.J. **1990**. The effect of summer tropical heating on the location and intensity of the extratropical westerly jet streams. Journal Geophysical Research, 95 (D11), pp. 18705–18721.

Yasuda T., **Hanawa** K. **1997**. Decadal changes in the mode waters in the mid-latitude North Pacific. Journal Physical Oceanography, Vol. 27, pp. 858–870.

Zhang Y., **Wallace** J.M. **1996**. Is climate variability over the North Pacific a linear response to ENSO? Journal of Climate, Vol. 9, pp. 1468–1478.

Zhang Y., Wallace J.M., Battisty D.S. **1997**. ENSO-like interdecadal variability: 1900–93. Journal of Climate, Vol. 10, pp. 1004–1020.